Acta Geotechnica (2021) 16:3177–3186
https://doi.org/10.1007/s11440-021-01144-6

RESEARCH PAPER

Efficient approach in modeling the shear strength of unsaturated soil using soil water retention curve

André Luís Brasil Cavalcante[1] · Pedro Victor Serra Mascarenhas[1]

Received: 15 May 2020 / Accepted: 8 January 2021 / Published online: 19 June 2021

Abstract
Currently, there are debates on the relationship between the effective stress and shear strength of unsaturated soils. Thus, it is imperative to present an efficient method that could contribute to the existing knowledge in this aspect while ensuring an easy and fast operation. In this study, a novel approach for modeling the shear strength of unsaturated soils using soil water retention curve (SWRC) is proposed. The method considers a coherent thermodynamic expression of Bishop's effective stress parameter χ and a physical model of the SWRC that depends only on one parameter. First, an expression for unsaturated effective stress was obtained. The starting point to develop the shear strength equation was then determined. The obtained equation can estimate Bishop's parameter for unsaturated soil using only the SWRC and the relationship between unsaturated shear strength and soil suction. A sensitivity analysis and comparison with other methods that obtained different parameter expressions were also provided. The results showed that the results obtained from the proposed model fits with experimental data, indicating its applicability in studying the average behavior of unsaturated sands.

Keywords SWRC · Unsaturated shear strength · Unsaturated soils · Water infiltration

1 Introduction

The relationship between the effective stress and shear strength of soils is a well-established concept in representing the standard stress state in classical soil mechanics. However, this relationship for unsaturated soils remains a central subject of several debates.

Among the main topics of these debates, a special spot is reserved to the Bishop's [3] effective stress equation. This is a widely used equation that generalizes the concept of effective stress in classical soil mechanics. The Bishop's [3] effective stress is:

$$\sigma' = (\sigma - u_a) + \chi(u_a - u_w) \quad (1)$$

where σ is the total soil stress [$ML^{-2}\ T^{-2}$], $\sigma^{-2}\ T^{-2}$], χ is the unsaturated effective stress parameter or Bishop's [3] parameter [non-dimensional], u_w is the pore water pressure [$ML^{-2}\ T^{-2}$], and u_a is the pore air pressure [$ML^{-2}\ T^{-2}$]. The main critics of Eq. (1) question the validity of χ [25]. Particularly, the uniqueness of χ must be clarified, and its experimental determination is difficult. Eventually, χ was found to be related to air entry pressure [2–19]. The Bishop's parameter χ is useful in the constitutive framework of critical state soil mechanics modeling.

Several authors proposed expressions that create a suitable fit for the experimental results for χ. The most successful expressions considered the soil microstructure and consequently, the soil water retention curve (SWRC) [1]. Xu and Cao [36] presented a list of the most successful expressions for χ, as shown in Table 1. In addition, there have been several proposed stress state frameworks for unsaturated soils [25]. Fredlund and Rahardjo [14] noted that the stress state of unsaturated soils should be described by two independent stress variables, typically the net stress and suction, that could be experimentally validated through a null test. Houlsby [18] indicated thermodynamics as the theoretical background of this two-stress-variable approach. By writing the work equation for the soil components, the possible pairs of stress state variables and

✉ André Luís Brasil Cavalcante
abrasil@unb.br

[1] Department of Civil and Environmental Engineering, University of Brasília, Brasília, DF 70910-900, Brazil

Table 1 Expressions for the unsaturated effective stress parameter [36]

Expressions	Authors
$\chi = K^n/K^{Sn}$	Chen et al. [10]
$\chi = 1/(1 + du_s)$	Röhm and Vilar [27]
$d =$ fitting parameter	
$\chi = S^{\kappa}$	Vanapalli et al. [32]
$\kappa =$ fitting parameter	
$\chi = u_s^{0.55}$	Khalili and Khabaz [20]
$\chi = (u_s/u_{se})^{D-3}$	Xu [35]
$\chi = S$	Schreffer [28]; Chaney et al. [9]; Sun et al. [31]
$\chi = S_e$	Lu et al. [23] Vanapalli et al. [32]; Xu and Cao [36]

conjugate strain variables could be determined. The hypotheses of Houlsby's derivation [18] are yet to be investigated and its consequences are yet to be fully understood [25]; however, this derivation provides a consistent thermodynamic approach in dealing with unsaturated effective stresses, which was useful for works that followed. This includes the possibility of applying a solid theoretical background to Bishop's effective stress expression [3].

Lu et al. [23] proposed a closed-form equation for the effective stress in unsaturated soils. They hypothesized that suction stress consumes most of the change in free energy. Starting from the suction stress retention curve and thermodynamic arguments, they additionally found an expression that relates to χ:

$$\chi = \frac{S - S_r}{1 - S_r} \tag{2}$$

where S is the degree of saturation [non-dimensional] and S_r is the residual degree of saturation [non-dimensional].

A major reason for choosing simple expressions, such as Eq. (2), is its suitability in modeling the general 3D boundary value stress–strain behavior of unsaturated soils. Particularly, constitutive models with χ have difficult implementation [30].

Recently, there have been other stress frameworks proposed for unsaturated soils. Duan et al. [12] proposed a generalized stress framework that considers the six different phase composition of soil: grain skeleton, cement, solid water, liquid water, contractile skin, and pore air. This new framework proposed a space- and time-dependent stress that can model the collapse phenomenon. The resulting generalized stress distinguishes the effects of the external loads and bonding properties of the bearing structure with the grain skeleton as the core.

Equation (2), also referred to as the normalized degree of saturation, plays an important role in determining the shear strength of unsaturated soils, which is the ability of soil to resist shear stress caused by the deviation of the stress state from the hydrostatic condition. There are two different approaches in treating the stress state variables for unsaturated soils [33]. The first approach consists of the same stress partitioning approach that employs the effective stress as the governing stress state of unsaturated soil, as proposed by Bishop [3]:

$$\tau = c' + [(\sigma - u_a) + \chi(u_a - u_w)] \tan \phi' \tag{3}$$

where c' is the effective cohesion [ML^{-2} T^{-2}], σ-u_a is the net normal stress [ML^{-2} T^{-2}], u_a-u_w is the matric suction [ML^{-2} T^{-2}], ϕ' is the angle of internal friction [non-dimensional], and τ is the unsaturated shear strength [ML^{-2} T^{-2}]. The second approach is based on the independent stress state variables proposed by Fredlund et al. [13]:

$$\tau = c' + (\sigma - u_a) \tan \phi' + (u_a - u_w) \tan \phi^b \tag{4}$$

where ϕ^b is the angle indicating the rate of increase in shear strength relative to the matric suction $(u_a - u_w)$ [non-dimensional].

Vanapalli [33] discussed the applications and development of different unsaturated shear strength models in geotechnical engineering practice. Although there are essentially different perspectives on the shear behavior of unsaturated soils, Eqs. (3) and (4) have been widely used and present proper compliance with experimental results [33]. These approaches can be essentially treated as equivalent with assumption of the following equality:

$$\chi = \frac{\tan \phi^b}{\tan \phi'} \tag{5}$$

Lu et al. [23] applied van Genuchten's [17] SWRC model in Eq. (2), resulting in the expression:

$$\chi = \left\{ \frac{1}{1 + \left[\alpha_{vg}(u_a - u_w)\right]^{n_{vg}}} \right\}^{1-1/n_{vg}} \tag{6}$$

where α_{vg} and n_{vg} are the fitting parameters [non-dimensional].

Different SWRCs could obtain different expressions for χ [23]. A problem in determining χ is the fit to the experimental data of the SWRC. Cavalcante and Zornberg's SWRC model [7, 8] uses minimum adjusting parameters to ensure the fit of the experimental data. This model adjusts the SWRC by obtaining an expression for Richards equation analogous to the advection–dispersion problem, which can be analytically solved. Their underlying hypotheses assumes that the following expressions are constant [7, 8]:

$$\frac{\partial k}{\partial \theta} = cte = \overline{a}_s \tag{7}$$

$$\frac{k(\theta)}{\rho_w g}\frac{\partial \psi}{\partial \theta} = cte = \overline{D}_z \tag{8}$$

where $\overline{a}_s$ is the constant unsaturated advective seepage velocity [LT^{-1}], k is the unsaturated hydraulic conductivity function [LT^{-1}], θ is the volumetric water content [non-dimensional], $\overline{D}_z$ is the constant unsaturated water diffusivity [L^2T^{-1}], ψ is the total soil suction using atmospheric pressure as reference [$ML^{-2}\ T^{-2}$], ρ_w is the water specific mass [ML^{-3}], and g is the gravitational acceleration [LT^{-2}]. Consequently, the SWRC equation is:

$$\psi(\theta) = -\frac{1}{\delta}\ln\left(\frac{\theta - \theta_r}{\theta_s - \theta_r}\right) \tag{9}$$

where θ_s is the volumetric water content at saturation [L^3L^{-3}], θ_r is the residual volumetric water content [L^3L^{-3}], and δ is a fitting hydraulic parameter [$M^{-1}L^2T^2$].

Total suction is a measurement of the free energy of soil water [14], comprising two different parts, as shown in:

$$\psi = (u_a - u_w) + \pi \tag{10}$$

where π is the osmotic suction [$ML^{-2}\ T^{-2}$]. Matric suction is associated with the surface tension on the water meniscus. Meanwhile, osmotic suction is associated with the salt content and gradient in soil water. Normally, osmotic suction has negligible effect on the shear strength of soil [14]. In addition, the authors assumed that the shear strength component added by the unsaturated soil state is only attributed to the influence of matric suction. Thus, the terms "suction" and "matric suction" are used interchangeably in this paper.

Unsaturated effective stress and shear strength are the base concepts in unsaturated soil mechanics. They constitute frameworks for the mechanical behavior of soils under unsaturated conditions, despite the chosen stress state approaches. Borja and White [5], Sharma et al. [29], Raj and Sengupta [26], Wang et al. [34], Nguyen et al. [24], Liu et al. [22], and Li and Yang [21] applied unsaturated soil mechanics and these stress concepts. In addition, recently, there have been various frameworks proposed for the shear strength equation for unsaturated soils. In Zhai et al. [37], the additional adhesion between soil particles due to the meniscus is summed to the other terms in the shear stress equation through the elemental analysis of unsaturated soil volume. The meniscus due to soil suction causes two distinct effects: an additional net normal stress action on the soil skeleton and additional adhesion between soil particles.

This study aims to develop a shear strength model using the effective saturation equivalence to χ. The SWRC model proposed by Cavalcante and Zornberg [7, 8] was used in determining a simple shear strength equation for unsaturated soils that depends on only one adjusting parameter and uses the traditional Bishop's effective stress Eq. [3]. The resulting model has the advantages of easy operation and speed in generating results. A comparison using other SWRC models is also presented. We aim to use our proposed equation as the basis for unsaturated shear strength analysis of this work. In addition, novel approaches to obtain the unsaturated shear strength can be combined with the SWRC model employed in this work to generate other models of the unsaturated shear strength. These combinations will be left for future work.

2 Model derivation

First, it is necessary to cite the relationship between the volumetric water content and degree of saturation:

$$S = \frac{\theta}{\theta_s} \tag{11}$$

The volumetric water content can then be solved:

$$\theta = \theta_r + (\theta_s - \theta_r)\exp[-\delta|u_a - u_w|] \tag{12}$$

Substituting Eq. (11) to Eq. (12):

$$S = S_r + (1 - S_r)\exp[-\delta|u_a - u_w|] \tag{13}$$

Subsequently, χ can be written using Cavalcante and Zornberg's SWRC model [7, 8] as:

$$\chi = \exp[-\delta|u_a - u_w|] \tag{14}$$

Figure 1 shows the variations of χ with suction under different adjusting parameters using Cavalcante and Zornberg's SWRC model [7, 8].

By applying Eq. (14), Bishop's effective stress [3] (Eq. (1)) and unsaturated shear strength (Eq. (3)) equations

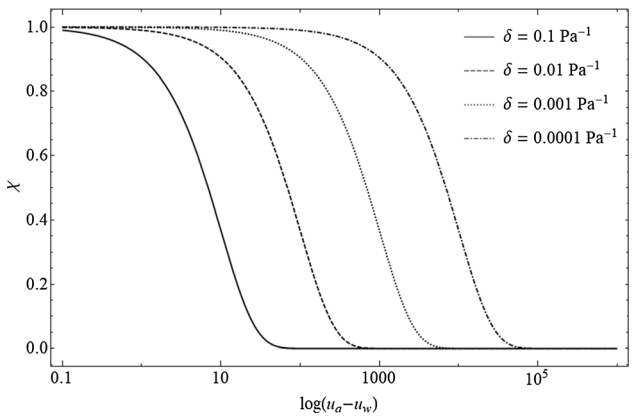

Fig. 1 Plot of χ versus $\log(u_a - u_w)$ for different values of the fitting hydraulic parameter δ

may be rewritten using Cavalcante and Zornberg's model [7, 8] as:

$$\sigma' = (\sigma - u_a) + e^{-\delta|u_a - u_w|}(u_a - u_w) \tag{15}$$

$$\tau = c' + [(\sigma - u_a) + e^{-\delta|u_a - u_w|}(u_a - u_w)] \tan \phi' \tag{16}$$

Figures 2 and 3 show the unsaturated effective stress and shear strength, respectively, at $\delta = 0.01$ Pa^{-1}, c' = 10 kPa, $\phi = 30°$.

Figure 3 shows the behavior of the unsaturated shear strength. For a given fixed net stress, shear strength initially increases with suction until reaching its peak value, which linearly depends on the net stress $u_a - {}_w$. Figure 4 shows the unsaturated shear strength using Eq. (16) for c' = 10 kPa and fixed net normal stress $\sigma - u_a = 30$ kPa.

After reaching the peak value, the effective stress, the following limit holds:

$$\lim_{\psi \to \infty} \tau = c + (\sigma - u_a)\tan(\phi) \tag{17}$$

The relation between the unsaturated shear strength and suction can then be divided into three main groups [15], as illustrated in Fig. 5.

The type of shear strength primarily depends on the granulometry:

- *Type I*: Shear strength increases to its peak value, after which it decreases to a residual fixed value. This is the typical relationship observed for sands, which have low chemical interaction between particles at the microscopic level.
- *Type II*: Shear strength increases to its peak value and thereafter remains approximately constant. This is the typical relationship observed for silt and some silty clays.

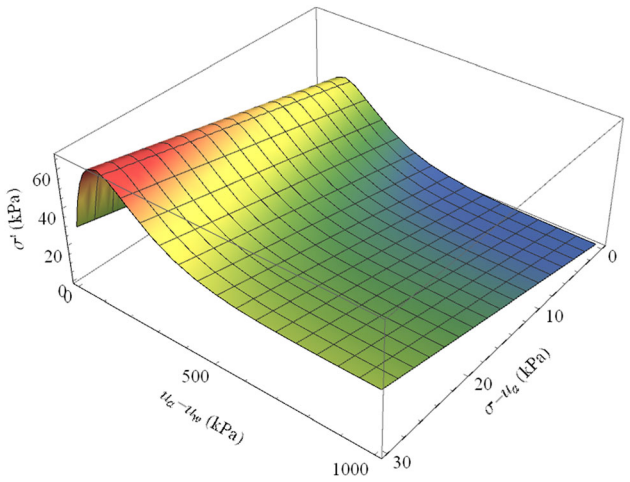

Fig. 2 Surface plot of the unsaturated effective stress varying with the net normal stress and matric suction

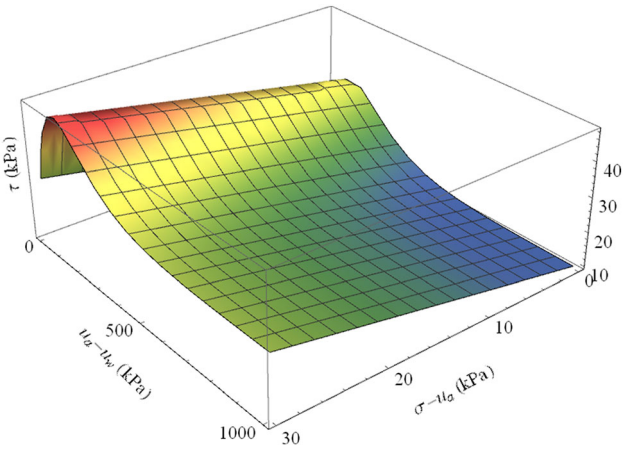

Fig. 3 Surface plot of the unsaturated shear strength varying with the net normal stress and matric suction

- *Type III*: Shear strength exhibits a monotonic increase with suction. This trend is typically observed in clays and some silty clays.

Considering the common types of shear strength curves, the combination of the equation of Lu et al. [23] for χ and Cavalcante and Zornberg's SWRC model [7, 8] results in a peak behavior. The unsaturated shear strength initially increases until it reaches its maximum value. Thereafter, it decreases until it reaches a residual value. This behavior of unsaturated shear strength is consistent with the type I shear strength in Fig. 5.

Due to suction decrease, the surplus soil strength due becomes negligible. When water content drops below a certain threshold, the decrease in water content reduces the cohesion bridges formed by the free water meniscus, resulting in the increased mobility of the soil particles.

The matric suction value where a peak occurs can be determined by obtaining the maximum value of the function. By calculating the derivative of Eq. (16) and equating it to zero, we found that:

$$(u_a - u_w)_{\text{peak}} = \frac{1}{\delta} \tag{18}$$

and

$$\tau_{\text{peak}} = \tan(\phi)\left[\frac{\exp(-1)}{\delta} + (\sigma - u_a)\right] + c' \tag{19}$$

In addition, Eq. (12) can be used to determine the volumetric water content at the peak unsaturated shear strength:

$$\theta = \theta_r + (\theta_s - \theta_r)\exp(-1) \tag{20}$$

Equation (20) allows the physical interpretation of the fitting hydraulic parameter δ. The fitting parameter is proportional to the initial slopes of the SWRC and unsaturated k-function of soil [7, 8]. Moreover, it is related to

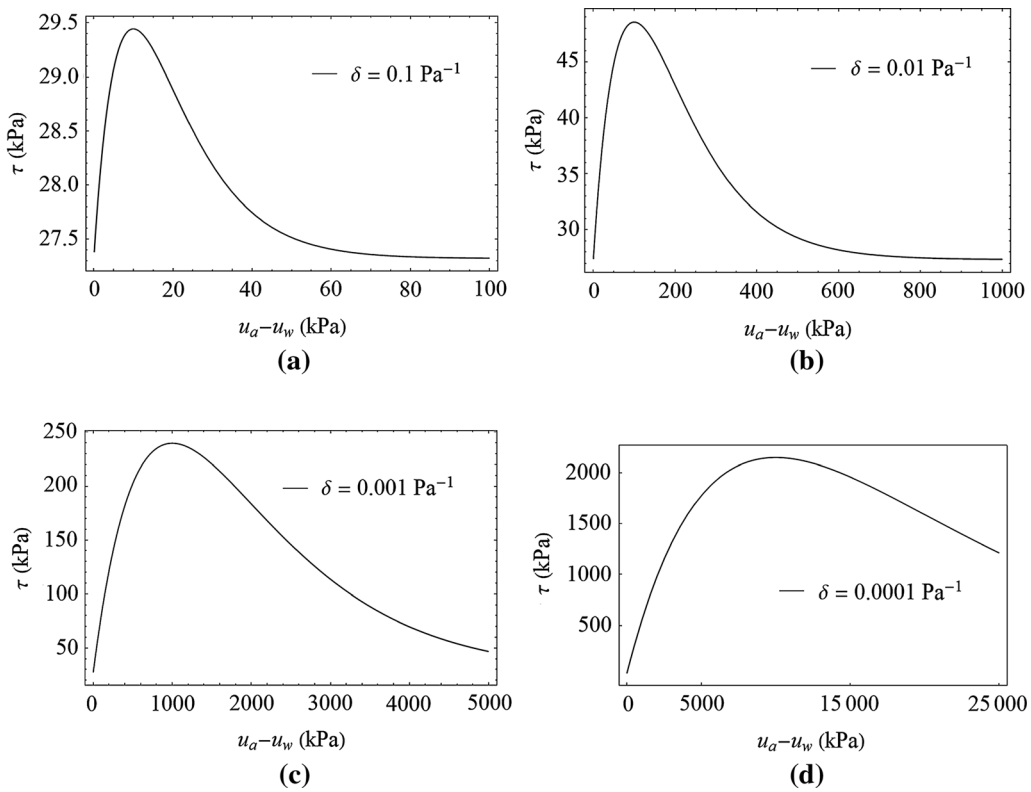

Fig. 4 Unsaturated shear strength using Eq. (16) at c' = 10 kPa and a fixed value of $\sigma - u_a$ = 30 kPa for: **a** δ = 0.1 $^{-1}$, **b** δ = 0.01 kPa^{-1}, **c** δ = 0.001 kPa^{-1}, and **d** δ = 0.0001 kPa^{-1}

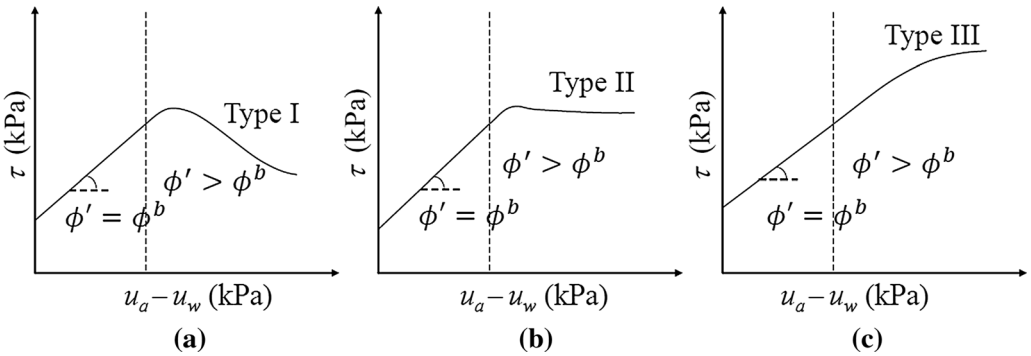

Fig. 5 Types of unsaturated shear strength behaviors (modified from Gao et al. [15]): **a** type I, **b** type II, and **c** type III

the air and water entry values. Particularly, a smaller value of the fitting parameter results in higher air and water entry values. Considering the new perspective posed by Eq. (20), it can be seen that δ is the immediate inverse of the suction value at which granular soils reach their maximum unsaturated shear strength.

Equation (18) shows the inverse relationship between the fitting hydraulic parameter and peak unsaturated shear strength. When δ decreases, air entry increases. As higher energy is required to remove the residual water that binds soil particles, the suction at the peak shear strength increases and shifts farther from the origin. In addition, small δ values could occur in soils with smaller average pore diameters, resulting in higher unsaturated shear strength values than those of soils with larger average pore diameters.

The shear strength model may be adapted to describe silt behavior as follows:

$$\tau = \begin{cases} c' + [(\sigma - u_a) + e^{-\delta|u_a - u_w|}(u_a - u_w)] \tan \phi', \\ u_a - u_w \leq 1/\delta \\ c' + \tan(\phi)\left[\dfrac{\exp(-1)}{\delta} + (\sigma - u_a)\right], \\ u_a - u_w > 1/\delta \end{cases} \tag{21}$$

For finer soils, such as silty clays and clays, which fit into type III shear strength, the deduced model is not recommended in predicting the shear strength behavior. Particularly, the microscopic chemical interaction between the soil particles for finer soils changes their shear strength curve, which does not decrease similar to that of sands. Thus, Eq. (16) can only be applied for low suction values in type III soil.

3 Unsaturated shear strength generated using other models

In this section, we compare the graphs generated using the SWRC model of Cavalcante and Zornberg [7, 8], and those of Gardner [16], Brooks and Corey [6], and van Genuchten [17] with the following equations, respectively:

$$\theta(u_a - u_w) = \theta_r + (\theta_s - \theta_r)\left[1 + \alpha_{r,g}(u_a - u_w)^{n_{r,g}}\right]^{-1} \tag{22}$$

$$\theta(u_a - u_w) = \theta_r + (\theta_s - \theta_r)\left[\alpha_{r,bc}(u_a - u_w)\right]^{-\lambda_{r,bc}} \tag{23}$$

$$\theta(u_a - u_w) = \theta_r + (\theta_s - \theta_r)\left\{1 + \left[\alpha_{r,vg}(u_a - u_w)\right]^{n_{r,vg}}\right\}^{-(1-1/n_{r,vg})} \tag{24}$$

where α [non-dimensional], λ [non-dimensional], and n [non-dimensional] are the fitting parameters for the SWRC models.

Using simple mathematical manipulation similar to Sect. 2, the corresponding expressions of Bishop's equation [3], unsaturated effective stress equation, and unsaturated shear strength equation using these three models can be obtained as:

$$\chi_g = \frac{1}{1 + \left[\alpha_{r,g}(u_a - u_w)\right]^{n_{r,g}}} \tag{25}$$

$$\chi_{bc} = \left[\frac{1}{\alpha_{r,vg}(u_a - u_w)}\right]^{\lambda_{r,bc}} \tag{26}$$

$$\chi_{vg} = \left\{\frac{1}{1 + \left[\alpha_{r,vg}(u_a - u_w)\right]^{n_{r,vg}}}\right\}^{1-1/n_{r,vg}} \tag{27}$$

Equations (25)–(27) can be combined with Eqs. (3) and (4) to generate unsaturated shear strength models.

The SWRC data were extracted from Azevedo [2], which was obtained using a lean clay soil from a burrow pit at Rocky Mountain Arsenal in Denver, CO. The SWRC curve was obtained by applying three different procedures: hanging column test, pressure plates, and thermodynamic methods. The measured data are illustrated in Fig. 6. Figure 7 shows the fitted models against the data presented in Fig. 6 obtained using Eqs. (22)–(24), respectively. By applying Eqs. (25)–(27), respectively, χ can be plotted against the matric suction using these models, as shown in Fig. 8.

By combining Eqs. (25)–(27) with Eq. (3), the following equations can be obtained:

$$\tau_g = c' + \left[(\sigma - u_a) + \frac{1}{1 + \left[\alpha_g(u_a - u_w)\right]^{n_g}}(u_a - u_w)\right]\tan\phi' \tag{28}$$

$$\tau_{bc} = c' + \left[(\sigma - u_a) + \left[\frac{1}{\alpha_{bc}(u_a - u_w)}\right]^{\lambda_{bc}}(u_a - u_w)\right]\tan\phi' \tag{29}$$

$$\tau_{vg} = c' + \left[(\sigma - u_a) + \left\{\frac{1}{1 + \left[\alpha_{vg}(u_a - u_w)\right]^{n_{vg}}}\right\}^{1-1/n_{vg}}(u_a - u_w)\right]\tan\phi' \tag{30}$$

By plotting Eqs. (28)–(30), the unsaturated shear strength surface plots for the models of Gardner [16], Brooks and Corey [6], and van Genuchten [17] can be obtained, as shown in Figs. 9, 10, 11, respectively.

Although Figs. 9, 10, 11 exhibit a trend similar to type III soils, their shear strength values differ. The variation of the shear strength with suction changes differs due to the differences in the SWRC models. Brooks and Corey's model [6] has the highest variation in shear strength due to suction, while Gardner's model [16] exhibits the smallest variation. Moreover, Lu et al. [23] showed that a peak behavior can be obtained for the effective stress in unsaturated soils for the van Genuchten's model [17] if $n > 2$. A similar peak behavior of the unsaturated shear stress is noted for $n > 2$. Thus, the unsaturated shear stress can be written as

$$\tau = c' + \sigma_{\text{bishop}}\tan\phi' \tag{31}$$

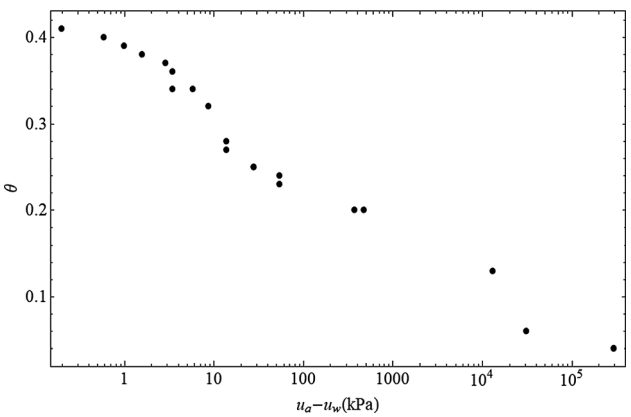

Fig. 6 SWRC data for lean clay soil from Azevedo [2]

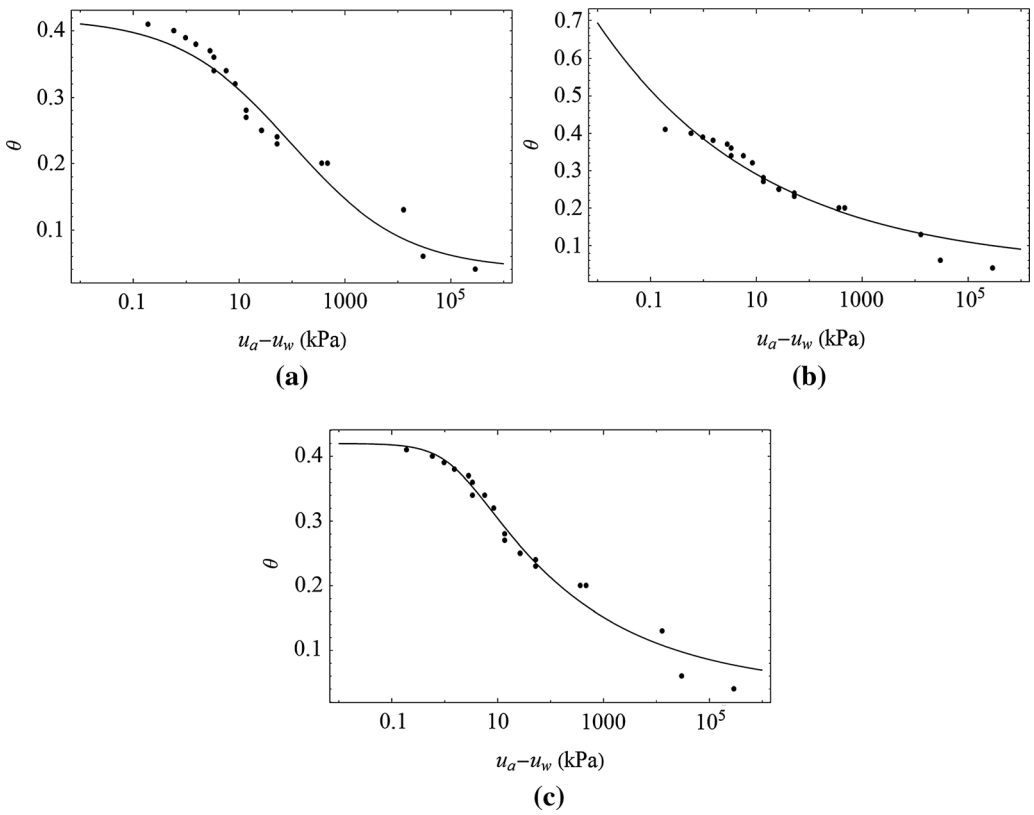

Fig. 7 SWRC models of **a** Gardner [16], **b** Brooks and Corey [6], and **c** van Genuchten [17], interpolated against the obtained SWRC curve of Azevedo [2]

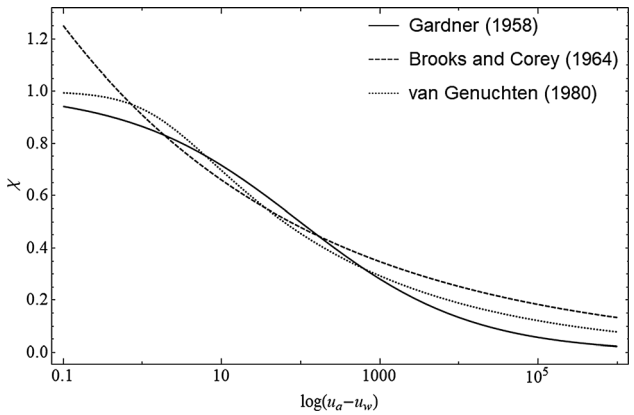

Fig. 8 Bishop's effective stress parameter (χ) [3] plotted against log ($u_a - u_w$) for the SWRC interpolated models

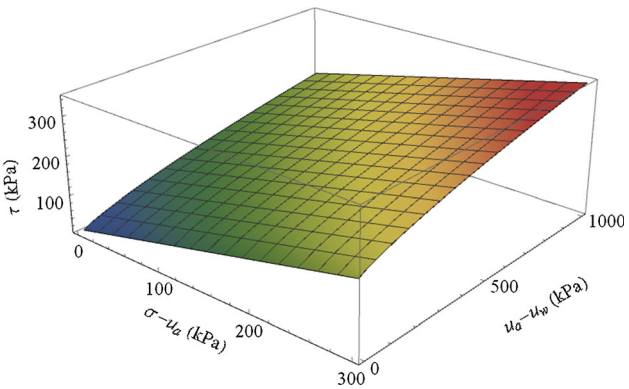

Fig. 9 Unsaturated shear strength surface plot using Gardner's SWRC model [16]

Because cohesion is assumed to be constant, the peak behavior for $n > 2$ under unsaturated effective stress implies a similar peak behavior in the unsaturated shear stress. Moreover, a similar peak condition is noted in Gardner's model [16] for $n > 2$, as demonstrated by the same procedure as in Lu et al. [23]. For $n = 2.5$ with the same fitting parameters, Figs. 12 and 13 show the variation of the unsaturated shear strength with suction using Gardner's SWRC model [16] and van Genuchten's SWRC model [17], respectively, for a fixed σ_{net} at 30 kPa, which was set for better visualization. It can be noted that the peak occurs at small suction values.

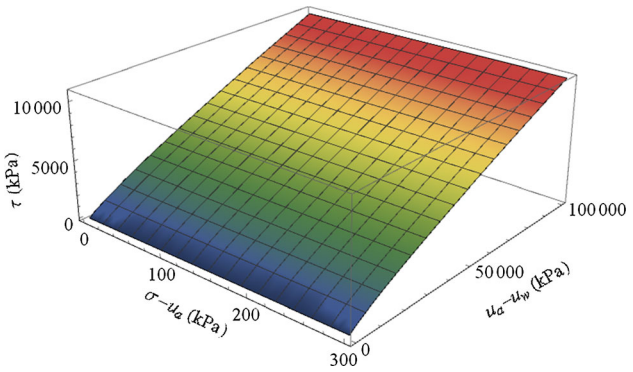

Fig. 10 Unsaturated shear strength surface plot using Brooks and Corey's SWRC model [6]

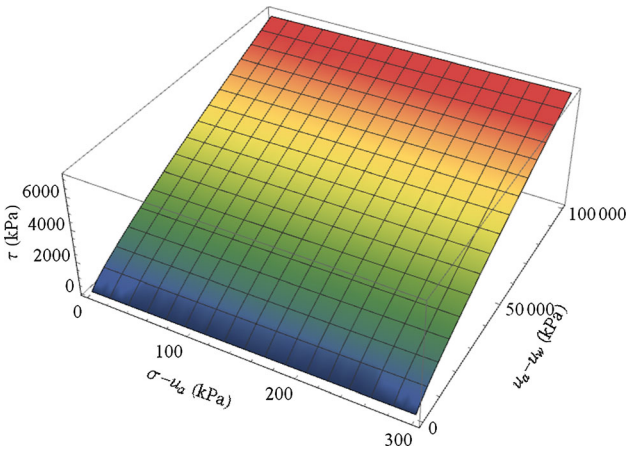

Fig. 11 Unsaturated shear strength surface plot using van Genuchten's SWRC model [17]

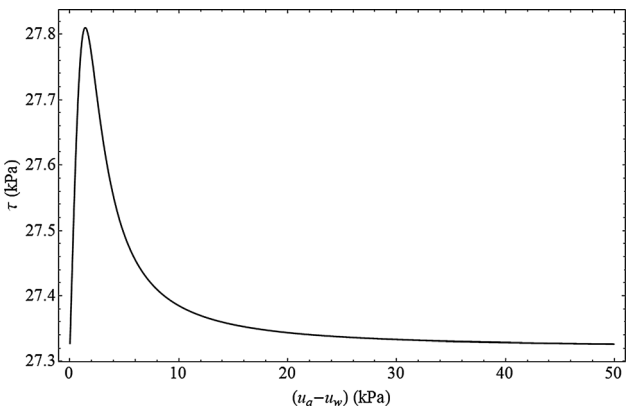

Fig. 12 Unsaturated shear strength versus suction using Gardner's SWRC model [16]

4 Application of the novel shear strength parameters

To illustrate the application of the model, a set of curves of the unsaturated shear strength versus suction for four different sands were adjusted using Eq. (16). The data were

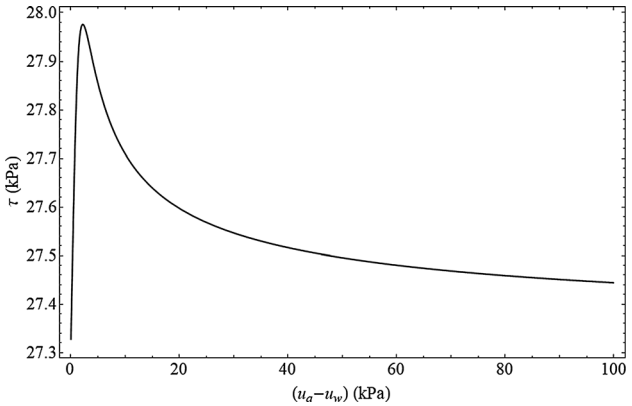

Fig. 13 Unsaturated shear strength versus using van Genuchten's SWRC model [17]

Table 2 Soil parameters for the sands studied [11]

Sand	Porosity (%)	σ_{net} (kPa)	ϕ'
Fine Frankston	52	9.2	34°
Graded Frankston	50	10.3	34°
Medium Frankston	47	10.45	33°
Brown Frankston	43	9.5	30°

extracted from Donald [11], which were collected from Frankston for four different graduated sand. The net normal stress and friction angle were measured in Donald [11], while δ and cohesion coefficient were adjusted from the model. Table 2 lists the soil parameters [11]. The results of the fitting are shown in Fig. 14, and the fitted parameters are listed in Table 3.

The results from Fig. 14 show that the fitting represents the change in the shear strength due to suction. As the model only exhibits minimal variations in the shear strength values, it is suitable for practical applications. Following curve fitting, hypothetical SWRCs can be generated using δ in the absence of further data. Assuming that θ_s is numerically equal to the porosity and $\theta_r = 0$, the results are shown in Fig. 15.

The proposed model is based on the Mohr–Coulomb failure criterion; thus, it does not comprise the compression effect on soils because the Mohr–Coulomb criterion accounts for perfect plastic failure, rather than the soil strain. Therefore, the model is not recommended for evaluating highly compressible soils when secondary stress–strain effects are expected to occur due to large strains. A one-dimensional perspective of the stress of unsaturated soils is used in validating the proposed model. For three-dimensional cases and stress tensor, the

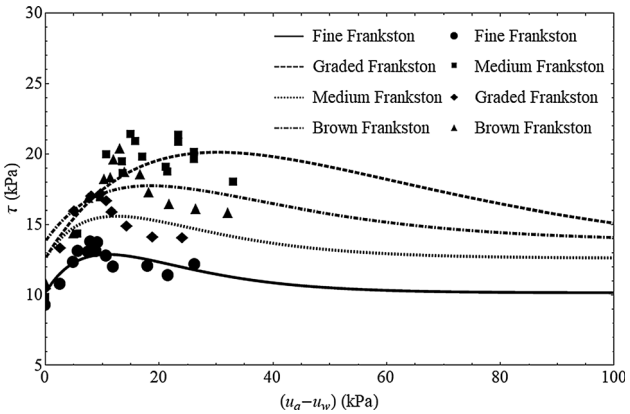

Fig. 14 Shear strength versus suction for the Frankston sands obtained by Donald [11]

Table 3 Fitted soil parameters

Sand	δ (kPa^{-1})	c' (kPa)
Fine Frankston	0.091	3.94
Graded Frankston	0.033	5.67
Medium Frankston	0.080	5.83
Brown Frankston	0.054	8.34

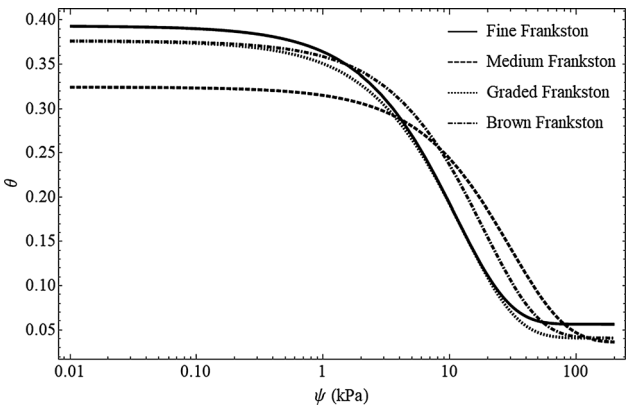

Fig. 15 Hypothetical SWRC for Frankston sands with the assumption that θ_s is numerically equal to the porosity and $\theta_r = 0$

underlying Mohr–Coulomb criterion must be generalized, which is not straightforward [4].

5 Conclusions

This study proposed a novel formula for Bishop's effective stress parameter [3] based on the SWRC model of Cavalcante and Zornberg [7, 8] and effective saturation expression of Lu et al. [23].

The resulting curves of the unsaturated shear strength agreed with those experimentally determined for sands and silty sands. In addition, the model can be adapted to simulate silt and some silty clays. However, it is not recommended for some silty clays and clays, except at low suction ranges. The proposed model was compared to strength models based on traditional SWRC equations. For the models of van Genuchten [17] and Gardner [16], promising results were obtained in modeling the shear strength versus matric suction. In contrast, Brooks and Corey's model [6] demonstrate some inconsistencies. For practical applications, the proposed model was used in representing the unsaturated shear behavior of sands. Careful analysis is required prior these actual applications in order to apply the model for a suited soil granulometry. Minimal variations were noted using the proposed model to determine the shear strength variation of Frankston sand, which can be safely disregarded in engineering practice.

For future works, the proposed equation can study unsaturated soil mechanics solutions for application in geotechnical engineering, such as slope stability analyses, foundation design, and retaining structural stability.

Acknowledgements This study was financed in part by the Coordination for the Improvement of Higher Education Personnel – Brasil (CAPES) – Finance Code 001. The authors also acknowledge the support of the National Council for Scientific and Technological Development (CNPq Grant 304721/2017-4 and 435962/2018-3), Foundation for Research Support of the Federal District (FAPDF) (Projects 0193.002014/ 2017-68 and 0193.001563/2017), CEB Geração S.A. (PD-05160-1904/2019), and University of Brasília.

Funding This study was financed in part by the Coordination for the Improvement of Higher Education Personnel – Brasil (CAPES) – Finance Code 001. The authors also acknowledge the support of the National Council for Scientific and Technological Development (CNPq Grant 304721/2017-4 and 435962/2018-3), Foundation for Research Support of the Federal District (FAPDF) (Projects 0193.002014/ 2017-68 and 0193.001563/2017), CEB Geração S.A. (PD-05160-1904/2019), and University of Brasília.

Availability of data and material All data and materials that support the findings of this study are available from the corresponding author upon reasonable request.

Compliance with ethical standard

Conflict of interest The authors have no relevant financial or non-financial interests to disclose.

Code availability All data, models, and code that support the findings of this study are available from the corresponding author upon reasonable request.

References

1. Alonso EE, Pereira J-M, Vaunat J, Olivella S (2010) A Microstructurally based effective stress for unsaturated soils. Géotechnique 60:913–925. https://doi.org/10.1680/geot.8.P.002
2. Azevedo MM (2016) Performance of geotextiles with enhanced drainage [Ph.D. thesis]. The University of Texas, Austin
3. Bishop AW (1959) The principle of effective stress. Tekn Ukeblad 106:859–863
4. Borja RI (2013) Plasticity Modeling & Computation. Springer, Berlin
5. Borja RI, White JA (2010) Continuum deformation and stability analyses of a steep hillside slope under rainfall infiltration. Acta Geotech 5:1–14. https://doi.org/10.1007/s11440-009-0108-1
6. Brooks R, Corey T (1964) Hydraulic properties of porous media. Hydrology Papers, 24. Colorado State University, p 37
7. Cavalcante ALB, Zornberg JG (2017) Efficient approach to solving transient unsaturated flow problems. I: Analytical solutions. Int J Geomech 17:04017013–14017011. https://doi.org/10.1061/(ASCE)GM.1943-5622.0000875
8. Cavalcante ALB, Zornberg JG (2017) Efficient approach to solving transient unsaturated flow problems II: Numerical solutions. Int J Geomech 17:04017014–14017011. https://doi.org/10.1061/(ASCE)GM.1943-5622.0000876
9. Chaney R, Demars K, Öberg A, Sällfors G (1997) Determination of shear strength parameters of unsaturated silts and sands based on the water retention curve. Geotech Test J 20:40–48. https://doi.org/10.1520/GTJ11419J
10. Chen ZH, Xie DY, Wang YS (1994) Effective stress in unsaturated soils. Chin Geotech Eng 16:62–69
11. Donald IB (1956) Shear strength measurements in unsaturated non-cohesive soils with negative pore pressures. In: Proceedings of the 2nd Australia–New Zealand Conference on Soil Mechanics and Foundation Engineering, Christchurch, new Zealand. Technical Publications Ltd., Wellington, New Zealand, pp 200–204
12. Duan X, Zeng L, Sun X (2019) Generalized stress framework for unsaturated soil: demonstration and discussion. Acta Geotech 14:1459–1481. https://doi.org/10.1007/s11440-018-0739-1
13. Fredlund DG, Morgenstern NR, Widger RA (1978) The shear strength of unsaturated soils. Can Geotech J 15:313–321. https://doi.org/10.1139/t78-029
14. Fredlund DG, Rahardjo H (1993) Soil mechanics for unsaturated soils. Wiley , NJ
15. Gao Y, Sun DA, Zhou A, Li J (2020) Predicting shear strength of unsaturated soils over wide suction range. Int J Geomech. https://doi.org/10.1061/(ASCE)GM.1943-5622.0001555
16. Gardner WR (1958) Some steady-state solutions of the unsaturated moisture flow equation with application to evaporation from a water table. Soil Sci 85:228–232. https://doi.org/10.1097/00010694-195804000-00006
17. van Genuchten MT (1980) A closed-form equation for predicting the hydraulic conductivity of unsaturated soils[1]. Soil Sci Soc Am J 44:892–898. https://doi.org/10.2136/sssaj1980.03615995004400050002x
18. Houlsby GT (1997) The work input to an unsaturated granula material. Géotechnique 1:193–196
19. Khalili N, Geiser F, Blight GE (2004) Effective stress in unsaturated soils: review with new evidence. Int J Geomech 4:115–126. https://doi.org/10.1061/(ASCE)1532-3641(2004)4:2(115)
20. Khalili N, Khabbaz MH (1998) A unique relationship for the determination of the shear strength of unsaturated soils. Géotechnique 48:681–687. https://doi.org/10.1680/geot.1998.48.5.681
21. Li Z, Yang X (2019) Three-dimensional active earth pressure for retaining structures in soils subjected to steady unsaturated seepage effects. Acta Geotech. https://doi.org/10.1007/s11440-019-00870-2
22. Liu HL, Wang CL, Kong GQ, Bouazza A (2019) Ultimate bearing capacity of energy piles in dry and saturated sand. Acta Geotech 14:869–879. https://doi.org/10.1007/s11440-018-0661-6
23. Lu N, Godt JW, Wu DT (2010) A closed-form equation for effective stress in unsaturated soil. Water Resour Res 46:1–14. https://doi.org/10.1029/2009WR008646
24. Nguyen VT, Tang AM, Pereira JM (2017) Long-term thermo-mechanical behavior of energy pile in dry sand. Acta Geotech 12:729–737. https://doi.org/10.1007/s11440-017-0539-z
25. Nuth M, Laloui L (2008) Effective stress concept in unsaturated soils: clarification and validation of a unified framework. Int J Numer Anal Meth Geomech 32:771–801. https://doi.org/10.1002/nag.645
26. Raj M, Sengupta A (2014) Rain-triggered slope failure of the railway embankment at Malda, India. Acta Geotech 9:789–798. https://doi.org/10.1007/s11440-014-0345-9
27. Röhm SA, Vilar OM (1995) Shear strength of an unsaturated sandy soil. Proc Int Conf Unsat Soils 1:31–38
28. Schrefler BA (1984) The finite element method in soil consolidation (with applications to surface subsidence) [Ph.D. thesis]. University College of Swansea
29. Sharma RH, Konietzky H, Kosugi KI (2010) Numerical analysis of soil pipe effects on hillslope water dynamics. Acta Geotech 5:33–42. https://doi.org/10.1007/s11440-009-0104-5
30. Song X, Borja RI (2014) Mathematical framework for unsaturated flow in the finite deformation range. Int J Numer Meth Eng 97:658–682. https://doi.org/10.1002/nme.4605
31. Sun DA, Sheng D, Xiang L, Sloan SW (2008) Elastoplastic prediction of hydro-mechanical behaviour of unsaturated soils under undrained conditions. Comput Geotech 35:845–852. https://doi.org/10.1016/j.compgeo.2008.08.002
32. Vanapalli SK, Fredlund DG, Pufahl DE, Clifton AW (1996) Model for the prediction of shear strength with respect to soil suction. Can Geotech J 33:379–392. https://doi.org/10.1139/t96-060
33. Vanapalli SK (2009) Shear strength of unsaturated soils and its applications in geotechnical engineering practice. In: Keynote address Proceedings of the 4th Asia-Pacific conference on Unsaturated Soils, pp 579–598
34. Wang J, Xiang W, Lu N (2014) Landsliding triggered by reservoir operation: a general conceptual model with a case study at three Gorges Reservoir. Acta Geotech 9:771–788. https://doi.org/10.1007/s11440-014-0315-2
35. Xu YF (2004) Fractal approach to unsaturated shear strength. J Geotech Geoenviron Eng 130:264–273. https://doi.org/10.1061/(ASCE)1090-0241(2004)130:3(264)
36. Xu Y, Cao L (2015) Fractal representation for effective stress of unsaturated soils. Int J Geomech. https://doi.org/10.1061/(ASCE)GM.1943-5622.0000446
37. Zhai Q, Rahardjo H, Satyanaga A, Dai G (2019) Estimation of unsaturated shear strength from soil–water retention curve. Acta Geotech 14:1977–1990. https://doi.org/10.1007/s11440-019-00785-y